Ann Nucl Med (2015) 29:697–708
DOI 10.1007/s12149-015-0993-3

ORIGINAL ARTICLE

Evaluation of semi-quantitative method for quantification of dopamine transporter in human PET study with ^{18}F-FE-PE2I

Yoko Ikoma[1] · Takeshi Sasaki[1] · Yasuyuki Kimura[1] · Chie Seki[1] · Yoshiro Okubo[2] · Tetsuya Suhara[1] · Hiroshi Ito[1,3]

Received: 27 March 2015 / Accepted: 16 June 2015 / Published online: 2 July 2015

Abstract
Objectives Positron emission tomography (PET) with ^{18}F-FE-PE2I is useful for investigating the function of dopamine transporter, and kinetics of ^{18}F-FE-PE2I could be described by standard two-tissue compartment model (2CM) using plasma input function. In this study, we investigated the feasibility of semi-quantitative methods for estimating binding potential (BP_{ND}) and transporter occupancy to shorten the scan period and to reduce the effect of statistical noise on quantitative outcomes using computer simulation and human PET studies with ^{18}F-FE-PE2I.
Methods In the simulations, time-activity curves (TACs) for the putamen with a wide range of BP_{ND} were generated. In these TACs, BP_{ND}s were estimated by standardized uptake value ratio (SUVR) using various integration intervals and the simplified reference tissue model (SRTM) with the cerebellum as reference region, and reduction of BP_{ND} assuming transporter occupancy by antipsychotics was calculated from BP_{ND} obtained from TACs with various BP_{ND} values. These estimates were evaluated by comparison with those of 2CM. In human studies with normal volunteers, BP_{ND}s were estimated in the caudate and putamen using SUVR and SRTM with the cerebellar reference region, and compared with BP_{ND} by standard 2CM.
Results In the simulations, BP_{ND} estimated by SUVR with late time frames and SRTM showed linear correlation with those by 2CM, although the estimates by SUVR were overestimated and affected by the cerebral blood flow as BP_{ND} became higher. As for transporter occupancy, SRTM showed higher linearity with 2CM and less effect of statistical noise than the SUVR method. In human studies, BP_{ND} by SRTM and SUVR with late time frames showed good correlation with BP_{ND} by 2CM.
Conclusions Although SRTM is more reliable than the SUVR method for BP_{ND} and occupancy estimation, SUVR using late time frames has the potential to provide practical indices of BP_{ND} and occupancy with a shorter scan period.

Keywords Positron emission tomography · ^{18}F-FE-PE2I · Binding potential · Standardized uptake value ratio (SUVR) · Occupancy

Introduction

Dopamine transporter (DAT) plays an important role in the regulation of dopamine concentration in the synaptic cleft, and DAT imaging with positron emission tomography (PET) demonstrated changes in the binding of DAT in neurodegenerative disorders and psychiatric disorders such as Parkinson's disease [1], Huntington disease [2], attention-deficit/hyperactivity disorder [3], and schizophrenia [4].

Recently, new PET ligands, *N*-(3-iodoprop-2*E*-enyl)-2β-carbomethoxy-3β-(4-methylphenyl)nortropane labeled with ^{11}C (^{11}C-PE2I) and a fluoroethyl analog of PE2I, ^{18}F-(*E*)-*N*-(3-iodoprop-2*E*-enyl)-2β-carbofluoroethoxy-3β-

✉ Yoko Ikoma
ikoma@nirs.go.jp

[1] Molecular Imaging Center, National Institute of Radiological Sciences, 4-9-1 Anagawa, Inage-ku, Chiba 263-8555, Japan

[2] Department of Neuropsychiatry, Nippon Medical School, 1-1-5 Sendagi, Bunkyo-ku, Tokyo 113-8602, Japan

[3] Advanced Clinical Research Center, Fukushima Medical University, 1 Hikariga-oka, Fukushima 960-1295, Japan

(4-methylphenyl)nortropane (^{18}F-FE-PE2I), were developed, and showed high affinity and good selectivity for DAT [5, 6]. Quantitative evaluation of ^{11}C-PE2I in humans has been performed using compartmental analysis with an arterial input function, graphical analysis, and a reference tissue model with the cerebellum as reference region, showing the possibility of quantifying binding to DAT in the striatum, thalamus, and also in the midbrain [4, 7–9]. However, those studies showed some limitations in terms of a reliable quantification in human studies with ^{11}C-PE2I; long scanning time is required due to slow kinetics in the striatum [10], and potentially brain-penetrating radioactive metabolites reported previously in rat brain [11] may be involved in total ^{11}C-PE2I binding in the brain.

^{18}F-FE-PE2I is a novel radioligand for DAT imaging, and PET studies in nonhuman primates demonstrated its faster kinetics and less production of radiometabolites penetrating the blood–brain barrier (BBB) compared with ^{11}C-PE2I [6]. Consequently, a direct comparison of the quantitative analyses of ^{11}C-PE2I and ^{18}F-FE-PE2I in nonhuman primates suggested that ^{18}F-FE-PE2I could be more suitable as a radioligand for in vivo quantification of DAT [12]. Recently, the quantification of DAT using ^{18}F-FE-PE2I was also evaluated in human brain of normal volunteers [13]. They reported that the kinetics of ^{18}F-FE-PE2I were well described by a standard two-tissue compartment model (2CM) using the parent radioligand in plasma as an input function if no major differences in metabolism between patients and controls are presented in clinical studies, and that noninvasive estimation of binding potential (BP_{ND}) by simplified reference tissue model (SRTM) with a 60-min scan would be sufficiently accurate for DAT quantification [13].

Quantitative analysis with 2CM or SRTM provides several physiological parameters including BP_{ND} that represent DAT density and affinity by nonlinear least-squares fitting method. On the other hand, semi-quantitative analysis using standardized uptake value ratio (SUVR), which is the ratio of radioactivity concentration between the target and reference regions at certain time frames after the injection, has often been applied to estimate BP_{ND} in PET receptor imaging [14]. This SUVR method is also useful in clinical research, and especially for patients who cannot lie on a bed for an extended period, as this analysis shortens the scan period and simplifies the estimation process. However, the reliability of BP_{ND} estimates depends on the time frames used for the calculation, and an optimal time frame for a reliable BP_{ND} estimation is dependent upon the kinetics of the radioligand. Therefore, it is important to validate whether the SUVR method reflects BP_{ND} in PET studies with ^{18}F-FE-PE2I.

In this study, we investigated the feasibility of the semi-quantitative method with SUVR as an index of DAT binding in human PET studies with ^{18}F-FE-PE2I using a computer simulation procedure and human data of normal volunteers.

Materials and methods

Theory

Estimation of binding potential

In this study, BP_{ND} was estimated by 2CM with an arterial input function, SRTM with a reference input function, and SUVR of the target and reference regions. SRTM and SUVR methods were evaluated as a simplified method, because they do not require the arterial blood sampling.

BP_{ND} estimates with two-tissue compartment model (BP_{2CM}) In time-activity curves (TACs) of the target and reference regions, each rate constant of the two-tissue compartment model (K_1, k_2, k_3, and k_4) is estimated by nonlinear least-squares fitting with an arterial input function, and BP_{ND} is calculated from the ratio of total distribution volume (V_T) between the target and reference regions as follows:

$$BP_{ND} = \frac{V_T^{tar} - V_T^{ref}}{V_T^{ref}} \quad (1)$$

$$V_T = \frac{K_1}{k_2}\left(1 + \frac{k_3}{k_4}\right), \quad (2)$$

where K_1 and k_2 are rate constants for the transfer from plasma to the non-displaceable compartment and from the non-displaceable compartment to plasma, respectively, and k_3 and k_4 represent the rate constants of association and dissociation for DAT, respectively. V_T^{tar} and V_T^{ref} are the total distribution volumes expressed as Eq. 2 of the target and reference regions, respectively. Note that BP_{ND} of the target region is not estimated directly as k_3/k_4 but is estimated indirectly with V_T of the target and reference regions, because the value of k_3/k_4 is unstable compared with V_T estimates.

BP_{ND} estimates with simplified reference tissue model (BP_{SRTM}) In the TAC of the target region, BP_{ND} is calculated by SRTM without an arterial input function, using instead the TAC of the reference region where specific bindings are negligible [15]. Parameters are estimated by nonlinear least-squares fitting with Eq. 3.

$$C_t(t) = R_1 C_r(t) + \left(k_2 - \frac{R_1 k_2}{1 + \mathrm{BP_{ND}}}\right) \times \exp\left(-\frac{k_2}{1 + \mathrm{BP_{ND}}} t\right) \otimes C_r(t)\,, \quad (3)$$

$$R_1 = \frac{K_1}{K_1^r}$$

where $C_t(t)$ and $C_r(t)$ are the radioactivity concentrations in the target and reference regions, respectively, and K_1 and K_1^r are the rate constants representing the transfer from plasma to the non-displaceable compartments of target and reference regions, respectively.

BP_{ND} estimates with standardized uptake value ratio (BP_{SUVR}) $\mathrm{BP_{ND}}$ is calculated from SUVR, which is the ratio of radioactivity concentration between the target and reference regions as follows:

$$\mathrm{BP_{ND}} = \frac{\int_{T_1}^{T_2} C_s(t)\mathrm{d}t}{\int_{T_1}^{T_2} C_{nd}(t)\mathrm{d}t} = \frac{\int_{T_1}^{T_2} (C_t(t) - C_{ref}(t))\mathrm{d}t}{\int_{T_1}^{T_2} C_{ref}(t)\mathrm{d}t}, \quad (4)$$

where C_{nd} and C_s are the radioactivity concentration of the non-displaceable and specifically bound radioligands in the target region, respectively, and C_t and C_{ref} are the total radioactivity concentrations of the target and reference regions, respectively. To estimate $\mathrm{BP_{ND}}$ without arterial input function, C_{nd} is replaced by C_{ref} on the assumption that the radioactivity concentration of the non-displaceable compartment in the target region is equal to the total radioactivity concentration in the reference region.

Estimation of transporter occupancy

Transporter occupancy represents the rate of DAT occupied by a drug such as an antipsychotic, and is calculated from the $\mathrm{BP_{ND}}$ of scans before and after taking the drug as follows [16]:

$$\mathrm{OCC}\ (\%) = \frac{\mathrm{BP_{base}} - \mathrm{BP_{drug}}}{\mathrm{BP_{base}}} \cdot 100, \quad (5)$$

where $\mathrm{BP_{base}}$ is the estimated $\mathrm{BP_{ND}}$ for the baseline scan, and $\mathrm{BP_{drug}}$ is the estimated $\mathrm{BP_{ND}}$ for the scan after taking the drug.

Simulation study

Reliability of binding potential estimates by simplified method

The feasibility of estimating $\mathrm{BP_{ND}}$ by simplified methods as a marker of DAT binding was investigated by computer simulation.

Generation of time-activity curves Time-activity curves for the putamen as target region, and the cerebellum as reference region, were simulated by deriving a dynamic tracer concentration for a 90-min scan from 2CM with a measured metabolite-corrected plasma TAC as an arterial input function and assumed k values obtained from a previously reported human study [13]. Although the putamen and caudate are targeted for evaluating the $\mathrm{BP_{ND}}$ in human studies, we generated only TAC of the putamen in this simulation, because the TACs derived from the caudate and putamen have a similar feature. In the putamen TACs, k_3 values were varied from 0.01 to 0.2 (1/min) at 0.01 intervals, corresponding to $\mathrm{BP_{ND}}$ values between 0.23 and 4.65, K_1 values were varied at 0.18, 0.22, 0.26, 0.30, and 0.34 (mL/mL/min), corresponding to the cerebral blood flow (CBF) values of 0.20, 0.28, 0.39, 0.55, and 0.85 (mL/mL/min) with fixed permeability and surface area product (PS = 0.434) obtained from K_1 and CBF values of normal volunteers [K_1 = 0.29(mL/mL/min), CBF = 0.5 (mL/mL/min)], and other parameters were fixed [K_1/k_2 = 4.25 (mL/mL), k_4 = 0.043 (1/min)]. Radioactivity concentrations of the non-displaceable radioligand [$C_{nd}(t)$] and specifically bound radioligand [$C_s(t)$] were calculated from the model equation of 2CM as well as the total radioactivity concentration in the target region ($C_t(t)$). Meanwhile, the cerebellum TAC was generated as the total radioactivity concentration in the reference region [$C_{ref}(t)$], in which k values were assumed as K_1 = 0.27 (mL/mL/min), k_2 = 0.14 (1/min), k_3 = 0.013 (1/min), and k_4 = 0.023 (1/min). In the cerebellum, although k_3 and k_4 estimated by the 2CM may not represent the specific binding but represent the non-specific binding or other components, these values were used to simulate the noiseless TAC of the cerebellum by the equation of 2CM.

Effect of binding potential on time course of $C_{nd}(t)$ In the SUVR method, it is not possible to obtain $C_{nd}(t)$ and $C_s(t)$ individually. Therefore, the TAC of the reference region [$C_{ref}(t)$] is substituted for $C_{nd}(t)$, and $C_s(t)$ is calculated by $C_s^{ref}(t) = C_t(t) - C_{ref}(t)$. To investigate the difference between $C_{nd}(t)$ and $C_{ref}(t)$, the time courses of $C_{nd}(t)$ and $C_s(t)$ with various k_3 values were compared with $C_{ref}(t)$ and $C_s^{ref}(t)$. Time of peak equilibrium, the time point at which $\mathrm{d}C_s(t)/\mathrm{d}t = 0$, was estimated from $C_s(t)$ and also from $C_s^{ref}(t)$, and the radioactivity ratio was calculated by C_s/C_{nd} or C_s^{ref}/C_{ref} at the peak equilibrium time.

Error of binding potential estimated by simplified method For each TAC, the $\mathrm{BP_{ND}}$ value was estimated by SUVR, SRTM, and 2CM. In the SUVR method, $\mathrm{BP_{SUVR}}$ was calculated by Eq. 4 from the accumulated radioactivity

for frames of early, middle, and late times; they were between 20 and 40 min (BP_{SUVR20}), between 40 and 60 min (BP_{SUVR40}), and between 70 and 90 min (BP_{SUVR70}). First, the reliability of BP_{ND} estimates by each simplified method was investigated in TACs with various k_3 values by comparing BP_{ND} by 2CM. Next, the effect of change in CBF of the putamen on BP_{ND} estimates was investigated, as it is possible that the CBF in the putamen might be different from that in the cerebellum due to neurologic or psychiatric diseases. In TACs with various K_1 values, the relationship between the BP_{ND} estimates by each simplified method and that by 2CM was examined.

Error of transporter occupancy estimated by simplified method The reliability of occupancy estimation in ^{18}F-FE-PE2I studies was investigated for each simplified method using the simulated TACs mentioned above. For each TAC set with the same K_1 value and various k_3 values [0.01 to 0.13 (1/min) at 0.01 intervals], OCC was calculated by Eq. 5 from BP_{ND} estimated by each simplified method; they are BP_{SRTM} (OCC_{SRTM}), BP_{SUVR20} (OCC_{SUVR20}), BP_{SUVR40} (OCC_{SUVR40}), BP_{SUVR70} (OCC_{SUVR70}), and compared with that from BP_{2CM} (OCC_{2CM}). In this calculation, the TAC with $k_3 = 0.13$ was used as the baseline scan, and the TACs with smaller k_3 ($k_3 = 0.01$–0.12) were assumed to be the scans after taking various drug doses.

Effect of statistical noise on binding potential estimates

The effect of statistical noise in the TACs on BP_{ND} estimates and transporter occupancy was investigated with noise-added simulated TACs for several BP_{ND} values. A dynamic tracer concentration for ^{18}F-FE-PE2I was obtained with 2CM and the measured input function mentioned above with the rate constants given as true values ($K_1 = 0.29$, $K_1/k_2 = 4.25$, $k_3 = 0.13$, $k_4 = 0.043$ for the putamen, and $K_1 = 0.27$, $k_2 = 0.14$, $k_3 = 0.013$, $k_4 = 0.023$ for the cerebellum). The value of k_3 in the putamen was varied at 0.06 and 0.02 assuming the conditions after taking the drug, so that the transporter occupancy calculated from BP_{2CM} would be approximately 50 % and 80 % from the baseline scan ($k_3 = 0.13$). The Gaussian distributed mean-zero noise with variance proportional to the true count was added to the non-decaying tissue activity for each frame using Eq. 6 [17]:

$$\sigma = F \cdot \sqrt{\frac{C_t(t_i)}{e^{-\lambda t_i} \cdot \Delta t_i}}, \quad (6)$$

where i is the frame number, C_t is the non-decaying tissue radioactivity concentration derived from the rate constants and the input function, t_i is the midpoint time of the i'th frame, Δt_i is the data collection time of the i'th frame, λ is the radioisotope decay constant, and F is a scaling factor representing the sensitivity of the measurement system that was introduced here to adjust the noise level. It should be noted that this equation assumes that noise, which is added to the TAC, is determined by the count of the curve itself. In fact, noise is determined by the total counts in the slice. In this simulation study, F was set so that the mean noise level from 1 to 90 min in the baseline scan would be 1, 3, 5, 7, 10, and 15 %, and 1000 noisy datasets were generated for each noise level.

In these simulated TACs for the putamen, BP_{ND}s were estimated by the SUVR method and also SRTM with various scan lengths of 90 min, 60 min, and 52 min. Parameter estimates were considered outliers if BP_{ND} was outside the range $0.0 < BP_{ND} < 9.0$, and the reliability of BP_{ND} estimates was evaluated by the mean and coefficient of variation [COV; sd/mean (%)] of the BP_{ND} estimates excluding outliers. In addition, transporter occupancy was calculated from estimated BP_{ND}s for each TAC using Eq. 5. The relationship between the reliability of BP_{ND} or transporter occupancy estimates and noise level was investigated for each simplified method. Note that statistical noise was added only to the putamen TAC, not to the cerebellum TAC, because generally the cerebellum TAC is derived from the region of interest (ROI) that is large enough to obtain noiseless TAC.

All simulation analyses were carried out using Matlab (The Mathworks, Natick, MA, USA).

Human study

Subjects

In this study, evaluation of the quantification method was performed for ten healthy men (mean age ± SD, 28.1 ± 6.9 years; age range 20–39 years) reported previously [13]. All subjects were free of any somatic, neurologic, or psychiatric disorders. The study was approved by the Ethics and Radiation Safety Committee of our institution. Written informed consent was obtained from all subjects before their inclusion in the study.

PET procedure

PET studies were performed on an ECAT EXACT HR+ (CTI-Siemens, Knoxville, TN, USA), which provides 63 planes and a 15.5-cm axial field of view. A 10-min transmission scan was acquired before an emission scan using a 3-rod source of ^{68}Ge–^{68}Ga for subsequent attenuation correction. Emission data were acquired over 90 min (9 × 20-s frame, 5 × 60-s frame, 4 × 120-s frame,

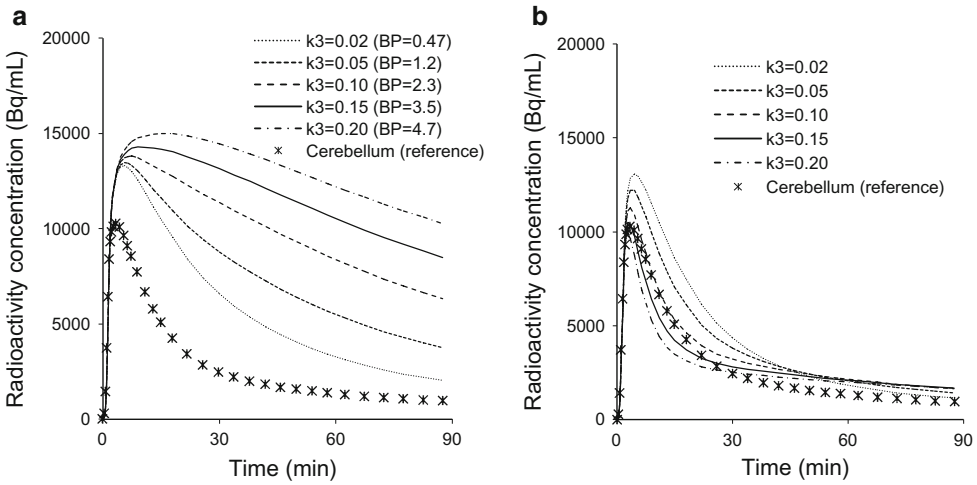

Fig. 1 Simulated time courses of $C_t(t)$ (**a**) and $C_{nd}(t)$ (**b**) for the target region with various k_3 values and the cerebellum used as reference region

11 × 240-s frame, and 6 × 300-s frame) in 3-dimensional mode after a bolus injection of 180.0 ± 9.3 MBq of ^{18}F-FE-PE2I synthesized as reported previously [18]. The specific radioactivity was 146.1 ± 98.7 GBq/μmol at the time of injection. The data were reconstructed by a filtered back-projection using Hanning filter (6.3 mm of full width at half maximum). Voxel size of the reconstructed images was 2.68 mm × 2.68 mm × 2.425 mm.

Arterial blood sampling and metabolite analysis were carried out as reported previously [13] to obtain a metabolite-corrected plasma TACs as an arterial input function.

T1-weighted MR images were acquired with a 1.5-T MRI scanner (Gyroscan NT; Philips) (1-mm-slice axial images; repetition time 21 ms; echo time 9.2 ms; flip angle 30°).

Data analysis

Individual MR images were coregistered to the corresponding PET images summed for all frames, and ROIs were defined manually on the coregistered MR images for the caudate, putamen, and cerebellum. The respective TACs were then extracted from the dynamic PET images. For each TAC of the caudate and putamen, BP_{ND} was estimated by 2CM with a metabolite-corrected arterial input function, SRTM using the cerebellar input function, and SUVR20, SUVR40, and SUVR70 using the cerebellum as reference region. In the 2CM, each rate constant was estimated by nonlinear least-square fitting with iteration of Marquardt algorithm without weighting and without constraints. The iteration was terminated when the relative changes of both Chi-square and the parameter with maximal change were smaller than 1 % for 5 times consecutively.

All human data analyses were carried out using PMOD (PMOD Technologies, Zurich, Switzerland).

Results

Simulation study

Reliability of binding potential estimates by simplified method

Figure 1 shows the simulated time courses of $C_t(t)$ and $C_{nd}(t)$ with various k_3 values and the TAC of the cerebellum used as reference region. The time course of $C_{nd}(t)$ differed depending on the k_3 value, and was different from the cerebellum TAC. In the time course of $C_s(t)$ simulated directly from the model equation with the plasma input function, peak equilibrium time was around 23 min, and it had little dependence on k_3 values (Fig. 2a, Table 1). The specific-to-free ratio ($=C_s(t)/C_{nd}(t)$) reached a plateau around 30 min (Fig. 2c), and this ratio at the peak equilibrium time well agreed with true BP_{ND} values (Table 1). Meanwhile, the time course of $C_s^{ref}(t)$ calculated with the reference region had a peak around 30 min when k_3 was large, and it became earlier as the k_3 value became smaller (Fig. 2b). The specific-to-free ratio obtained from $C_{ref}(t)$ and $C_s^{ref}(t)$ ($=C_s^{ref}(t)/C_{ref}(t)$) kept increasing even after 30 min when k_3 was large (Fig. 2d), and this ratio at peak equilibrium time or later differed greatly from the ratio obtained from $C_s(t)/C_{nd}(t)$ (Table 1).

The relationship between the BP_{ND}s estimated by the simplified methods and those by 2CM was investigated using TACs with various k_3 values and fixed K_1 value ($K_1 = 0.30$), as shown in Fig. 3. BP_{SRTM} showed a linear correlation with BP_{2CM}, although BP_{SRTM} was slightly underestimated as BP_{ND} became larger. BP_{SUVR70} was also linearly correlated with BP_{2CM}; however, BP_{SUVR70} was remarkably overestimated. Meanwhile, in BP_{SUVR20} and BP_{SUVR40}, the estimates dropped from a linear correlation as BP_{ND} became larger.

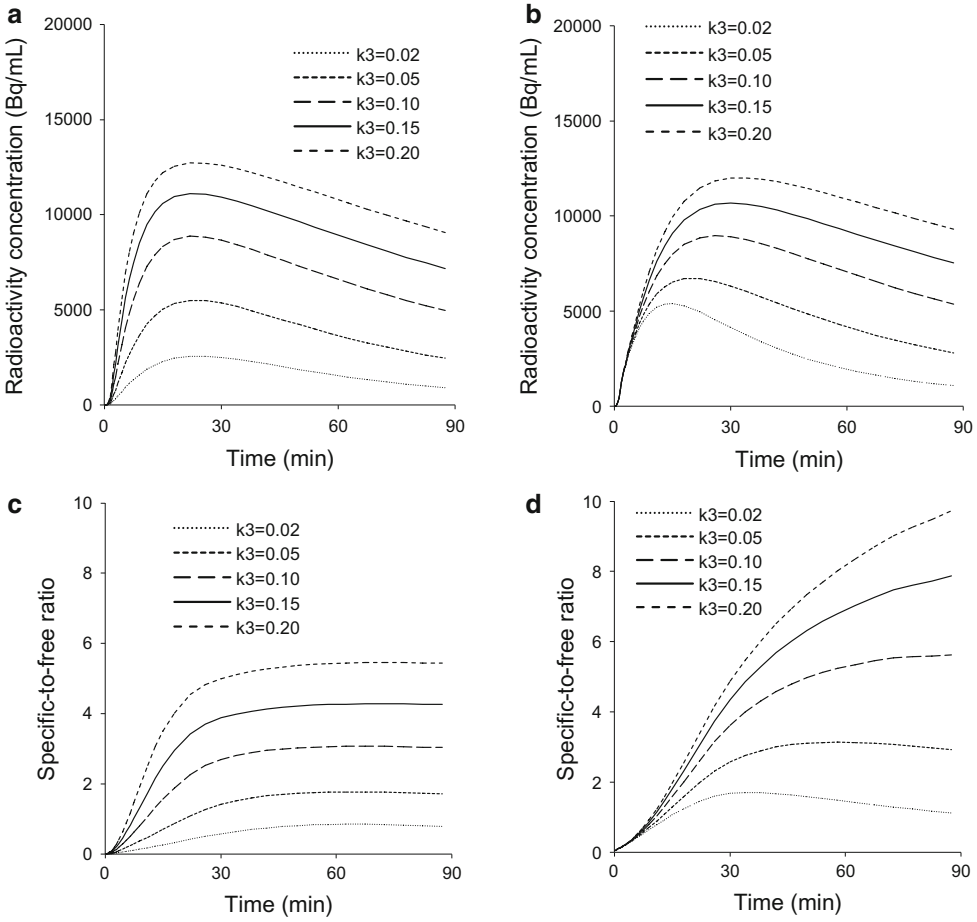

Fig. 2 Simulated time courses of $C_s(t)$ (**a**) and $C_s^{ref}(t)$ (**b**) and specific-to-free ratio obtained from $C_s(t)/C_{nd}(t)$ (**c**) and $C_s^{ref}(t)/C_{ref}(t)$ (**d**) for the target region with various k_3 values

The effect of CBF on BP_{ND} estimates by the simplified methods was investigated using the simulated TACs with various K_1 and k_3 values (Fig. 4). In all methods, BP_{ND} estimates became smaller as the K_1 value became lower, and the magnitude of BP_{ND} change caused by the K_1 value was larger in BP_{SUVR20} and BP_{SUVR40}, and smallest in BP_{SRTM}. BP_{SUVR70} and BP_{SRTM} did not change according to the K_1 values when the BP_{ND} value was small, but the effect of K_1 became larger as the BP_{ND} values increased.

In the occupancy estimation, OCC_{SRTM} agreed well with those from OCC_{2CM}, and the relationship did not depend on the K_1 values (Fig. 5d). Good agreement was also observed in OCC_{SUVR70}, although they were underestimated when the K_1 value was lower (Fig. 5c). On the other hand, OCC_{SUVR20} and OCC_{SUVR40} were much underestimated and did not show a linear correlation with OCC_{2CM}, and estimates were affected seriously by the K_1 values (Fig. 5a, b).

Effect of statistical noise on binding potential estimates

The relationship between BP_{ND} estimates and noise level was investigated for each simplified method (Fig. 6). In all methods, COV became larger as noise increased. For the TACs with $k_3 = 0.13$ assuming the baseline scan, by the noise level of ROI-based analysis, which was 1–5 % noise level, COV was within 5 % by all methods. In the noise level of voxel-based analysis, a 10–15 % noise level, COV of SUVR methods was still about 5 % and smaller than that of SRTM. COV of BP_{SRTM} was almost the same as BP_{SUVR70} when the scan length was 90 min. However, COV of BP_{SRTM} became remarkably larger as the scan length became shorter. The noise-induced bias of estimated BP_{ND} was within 1 % for all methods at the noise level of ROI-based analysis. At the noise level of voxel-based analysis, no noise-induced bias was observed in SUVR methods. Meanwhile, in the SRTM methods, the bias became larger as the noise increased.

On the other hand, for TACs with smaller k_3 assuming the scan after drug treatment, COVs of BP_{ND} estimated by the SUVR method became larger as the k_3 value became smaller, and they were higher than that of SRTM with 90-min scan. For TACs with $k_3 = 0.06$, COV of SRTM became larger than that of SUVR methods as the scan length became shorter than 60 min. COV of SUVR70 was 3.0 % at 5 %-noise level, and that of SRTM with 90- and 60-min scan was about 1.8 and 3.3 %, respectively. For TACs with

Table 1 Transient equilibrium time and BP_{ND} estimates at the transient equilibrium in the simulated time-activity curves with various k_3 values and fixed K_1 value ($K_1 = 0.30$)

	k_3 value of simulated curve (1/min)					
	0.02	0.05	0.10	0.13	0.15	0.20
True BP_{ND} ($=k_3/k_4$)	0.465	1.16	2.33	3.02	3.49	4.65
Simulated C_s						
Transient equilibrium time (min)	24.5	23.5	23	23	23	23.5
BP_{eq} ($=C_s/C_{nd}$)	0.467	1.16	2.33	3.04	3.50	4.66
Calculated C_s^{ref} with reference						
Transient equilibrium time (min)	15	22	26	30	30	34
BP_{eq} ($=C_s^{ref}/C_{ref}$)	1.07	1.97	3.16	4.08	4.34	5.48

BP_{eq} BP_{ND} value derived from the radioactivity ratio of specific-to-non-displaceable compartment at transient equilibrium time

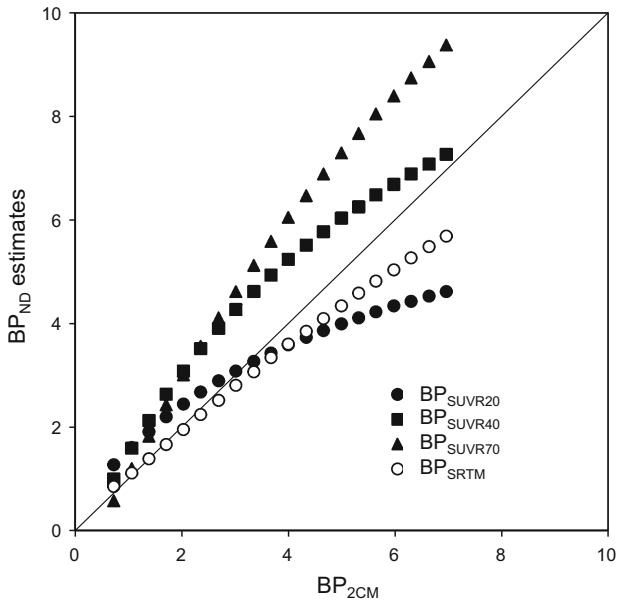

Fig. 3 Relationship between BP_{ND}s estimated by the simplified methods; SUVR20, SUVR40, SUVR70, SRTM, and those by the two-tissue compartment model (2CM) obtained from the simulated time-activity curves with various k_3 values ($K_1 = 0.30$, $k_3 = 0.01$–0.20)

$k_3 = 0.02$, COV of SRTM was smaller than that of SUVR methods even if scan length was 60 min. COV of SUVR70 was 6.1 % at 5 %-noise level, and that of SRTM with 90- and 60-min scans was about 1.9 and 2.3 %, respectively.

In the estimation of transporter occupancy, COV was smallest in the estimates by SRTM with 90-min data (Fig. 7). In COV of estimates by the SUVR methods, SUVR70 was smaller than SUVR20 and SUVR40, and its COV was almost the same as SRTM with 90-min data. Noise-induced bias was not observed in any of the methods.

Human study

Although BP_{SRTM} values for the caudate and putamen were slightly lower than BP_{2CM}, they showed good correlation with BP_{2CM} (putamen: $r = 0.92$, $p < 0.001$, caudate: $r = 0.93$, $p < 0.001$) (Fig. 8). BP_{SUVR70} was higher than BP_{2CM}, but it also showed good correlation with BP_{2CM} (putamen: $r = 0.82$, $p < 0.01$, caudate: $r = 0.86$, $p < 0.01$). Meanwhile, no correlation was observed between BP_{SUVR20} and BP_{2CM}.

Discussion

Binding potential estimates by SUVR method

The feasibility of the simplified methods for estimating DAT binding was investigated in order to shorten the scan period and to improve the reliability of quantitative outcomes in a PET study with ^{18}F-FE-PE2I. The most general simplified method is to calculate the ratio of radioactivity concentration between the target and reference regions as expressed in Eq. 4. By this SUVR method, the radioactivity concentration is summed for several frames to reduce the effect of the statistical noise in TACs, and the SUVR estimates depend on the time frames used for the integration of radioactivity concentration. Therefore, it is important to select an optimal time interval that reflects the binding potential.

In the SUVR method, TAC is generally integrated for a time interval that either embraces the time for peak equilibrium [19–21] or a late part of the scan [22–25]. In substitution for the secular equilibrium with a continuous infusion, the peak equilibrium with a bolus injection when $dC_s(t)/dt = 0$ was often applied, and theoretically, $C_s(t)/C_{nd}(t)$ represents k_3/k_4 at this peak equilibrium time [26]. In simulated TACs of ^{18}F-FE-PE2I, the time course of $C_s(t)$ showed a peak equilibrium around 23 min (Fig. 2a), and the peak equilibrium time hardly depended on the k_3 value. Estimated $C_s(t)/C_{nd}(t)$ at the peak equilibrium time was consistent with true BP_{ND} values (Table 1). However, BP_{SUVR20} calculated by Eq. 4 with frames from 20 to 40 min using the cerebellum as reference region did not agree with the true BP_{ND}s, and BP_{SUVR20} dropped from the linear correlation with BP_{2CM} as the k_3 value became larger

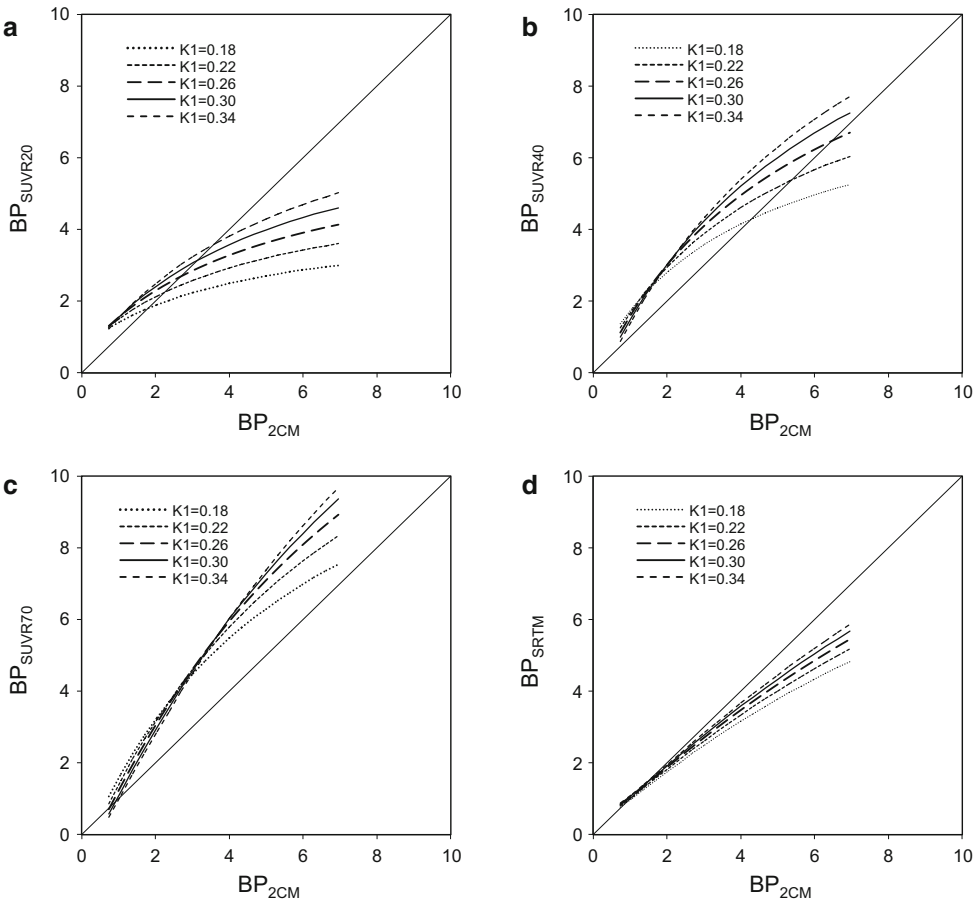

Fig. 4 Relationship between BP_{ND}s estimated by the simplified methods; SUVR20 (**a**), SUVR40 (**b**), SUVR70 (**c**), SRTM (**d**), and those by the two-tissue compartment model (2CM) obtained from the simulated time-activity curves with various K_1 and k_3 values ($K_1 = 0.18$–0.34, $k_3 = 0.01$–0.20)

(Fig. 3). By the SUVR method without an arterial input function, the radioactivity concentration of C_s and C_{nd} in the target region cannot be obtained independently. Therefore, the radioactivity concentration in the reference region (C_{ref}), where specific binding is negligible, is used as substitute for C_{nd}. However, strictly speaking, C_{ref} is often different from C_{nd} (Fig. 1b), resulting in a discrepancy between C_s and C_s^{ref}. In the simulations, the peak equilibrium time of C_s^{ref} changed according to the k_3 value, and it became later as the k_3 value became larger (Table 1). In addition, the specific-to-free ratio increased steeply around 30 min. Therefore, in TACs with a wide range of k_3 values, the SUVR method with a fixed time interval around the peak equilibrium time may cause errors in BP_{ND} estimates. Furthermore, the radioactivity concentration at early times is much affected by CBF change (Fig. 4), and thus, it would be difficult to estimate BP_{ND} reliably from the early frames including the peak equilibrium time.

On the other hand, in the SUVR method with late time frames for ^{18}F-FE-PE2I, the specific-to-free ratio C_s^{ref}/C_{ref} approaches a plateau around 70 min in the simulated TACs except those with extremely high k_3 value or low K_1 value (Fig. 2), and this was also observed in the human data reported previously [13]. However, the specific-to-free ratio around 70 min was much larger than that around 30 min, and especially in the TAC with a high k_3 value, resulting in the overestimation of BP_{SUVR70} in the simulated TACs and also in the human data (Figs. 4, 8). Although SUVR with late times cannot provide BP_{ND} itself, unlike BP_{SUVR20} and BP_{SUVR40}, BP_{SUVR70} had a good linear correlation with BP_{2CM} in both simulation and human data, and was little affected by the K_1 value within the possible range of K_1 for usual scans (Figs. 3, 4, 8). In addition, the half-life of ^{18}F is longer than that of ^{11}C, and thus, the statistical noise in the TAC is small enough to estimate SUVR reliably even 90 min after the injection in voxel-based estimation (Fig. 6). In this respect, BP_{SUVR70} would represent a practical index reflecting the change in BP_{ND} for clinical evaluation especially in regions with high BP_{ND}, such as the caudate and putamen.

In human data, BP_{SUVR70} and BP_{SRTM} showed a correlation with BP_{2CM}. However, BP_{SUVR70} was much higher than BP_{2CM}. Meanwhile, BP_{SRTM} became smaller than BP_{2CM} as the BP_{2CM} became large. These results are consistent with the result of simulation shown in Fig. 3. The correlation between the BP_{SUVR70} and BP_{2CM} was not strong as the correlation between the BP_{SRTM} and BP_{2CM}. This may be caused by variation of K_1 among individuals.

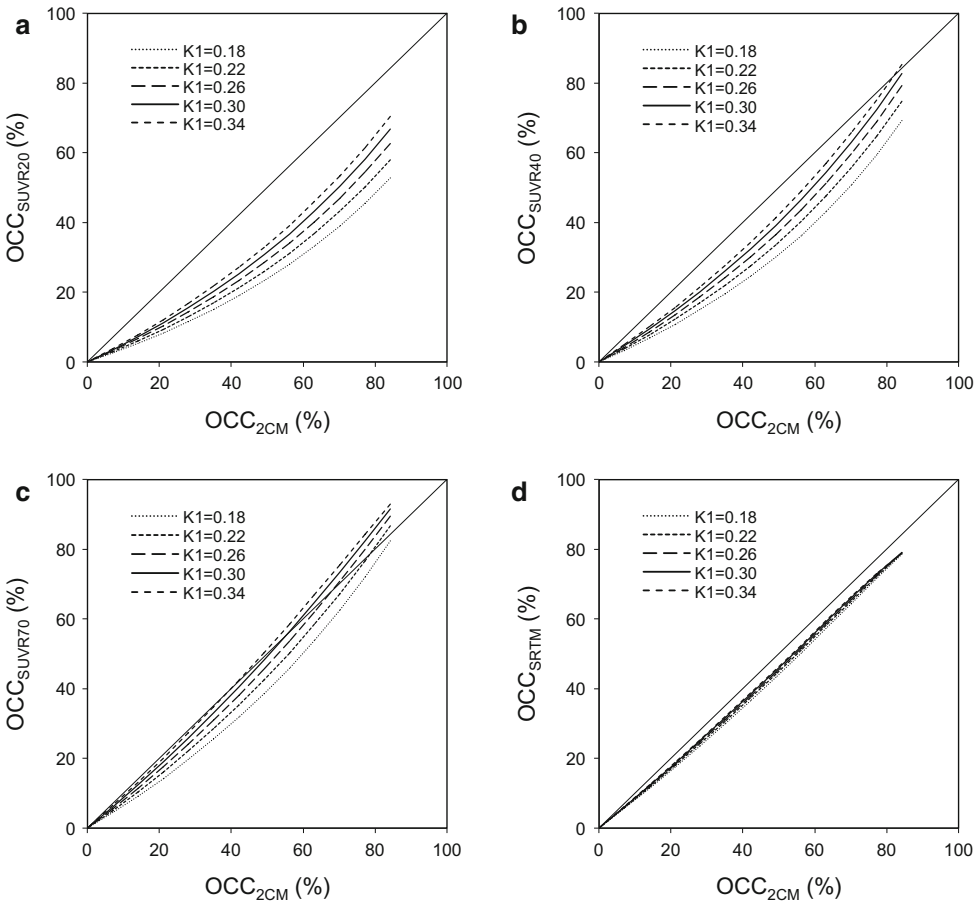

Fig. 5 Relationship between the occupancy obtained from BP_{ND} by SUVR20 (**a**), SUVR40 (**b**), SUVR70 (**c**), SRTM (**d**), and the occupancy obtained from the BP_{ND} by the two-tissue compartment model (2CM) estimated from the simulated time-activity curves with various K_1 and k_3 values ($K_1 = 0.18$–0.34, $k_3 = 0.01$–0.13)

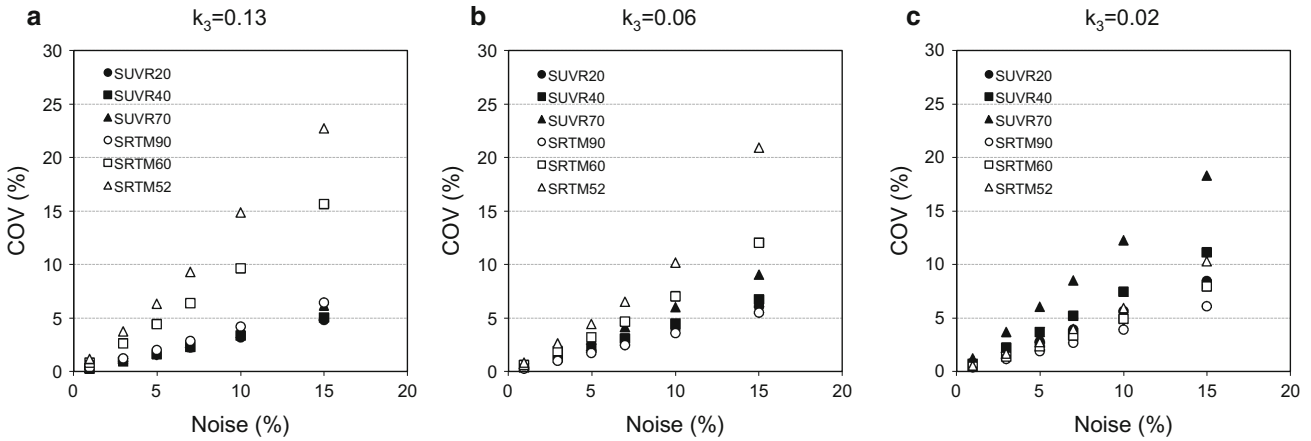

Fig. 6 Relationship between COV of BP_{ND} estimates and noise levels obtained from 1000 simulated time-activity curves with $k_3 = 0.13$ (**a**), $k_3 = 0.06$ (**b**), and $k_3 = 0.02$ (**c**) for each noise level at 1, 3, 5, 7, 10, and 15 %

Binding potential estimates by simplified reference tissue model

Another way to shorten the scan time is to reduce the scan length in the BP_{ND} estimation by SRTM. In the human data with ^{18}F-FE-PE2I, it has already been reported that BP_{ND} estimated by SRTM using data up to 60 min was well correlated with those by SRTM using data up to 90 min [13]. In our simulations, the result obtained from TACs without noise showed that the error of BP_{SRTM} estimates was small even in the estimation with data up to 45 min (data not shown). However, in the simulated TACs with

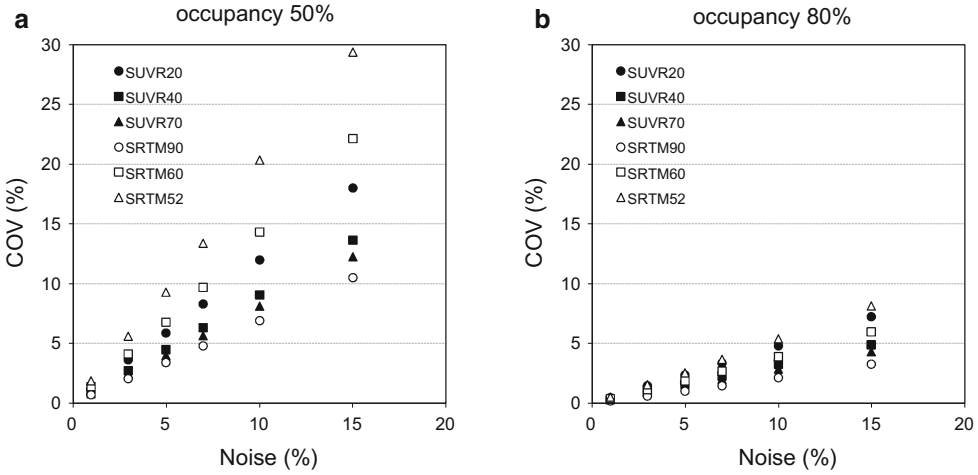

Fig. 7 Relationship between COV of occupancy and noise levels for time-activity curves with $k_3 = 0.06$ (about 50 % occupancy) (**a**) and $k_3 = 0.02$ (about 80 % occupancy) (**b**) obtained from 1000 simulated time-activity curves for each noise level at 1, 3, 5, 7, 10, and 15 %

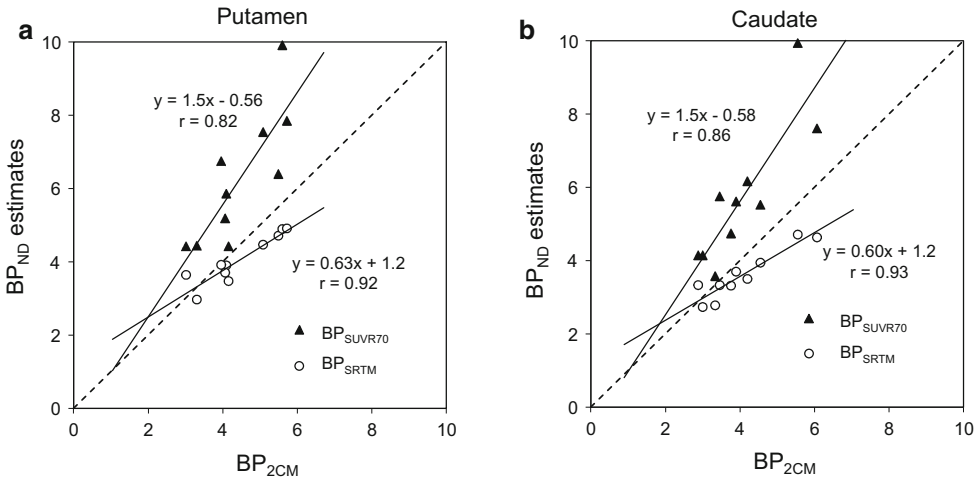

Fig. 8 Relationship between BP_{ND}s estimated by the simplified methods (SUVR70 and SRTM) and those by the two-tissue compartment model (2CM) for the putamen (**a**) and caudate (**b**) in human PET studies with ^{18}F-FE-PE2I

statistical noise, the bias and COV of BP_{SRTM} estimates became larger as the scan length became shorter. A 90-min scan is required to estimate BP_{ND} within the magnitude of COV, the same as the SUVR method, and a 60-min scan is acceptable for the estimation within 5 % COV at a noise level of 5 %, which is almost same as the noise level of caudate or putamen TAC. Meanwhile, for the voxel-based estimation, SRTM using data up to 60 min showed remarkably higher COV than SRTM using data up to 90 min as well as the SUVR method (Fig. 6). Therefore, it is difficult to shorten the scan length to less than 60 min for a stable estimation, and especially for a voxel-based estimation. BP_{SRTM} has good linearity with BP_{2CM}, and the effect of K_1 on BP_{ND} estimates was smaller than the SUVR methods, demonstrating better reliability as BP_{ND} estimates than the SUVR method. Meanwhile, from the viewpoint of scan length, BP_{SUVR70} would be a practical method because of the advantage of BP_{ND} being able to be provided with small noise-induced bias and small COV from the summation activity of only 20-min data, although it has a drawback that BP_{ND} is overestimated.

Estimation of transporter occupancy

BP_{SUVR20} and BP_{SUVR40} deviated from the linear correlation with BP_{2CM} as BP_{ND} increased, and this nonlinear correlation caused the bias of OCC_{SUVR20} and OCC_{SUVR40} in transporter occupancy estimation (Fig. 5). Compared with OCC_{SUVR20} and OCC_{SUVR40}, OCC_{SUVR70} showed better linearity with OCC_{2CM} and less effect of K_1 values, suggesting the usefulness of BP_{SUVR70} in the occupancy estimation. However, OCC_{SUVR70} became smaller as the K_1 value became lower. Therefore, OCC_{SUVR70} should be attempted with caution in case CBF in the target region decreases because of neurologic or psychiatric disease or the K_1 value would change among individuals. On the other hand, the occupancy estimated from BP_{SRTM} had good correlation with OCC_{2CM}, and they were not affected by K_1

values (Fig. 5). In addition, BP_{SRTM} was more reliable than BP_{SUVR70} when the k_3 value was smaller (Fig. 6), suggesting that the SRTM is suitable for the measurement of transporter occupancy in which the k_3 value has a wide range. However, the effect of statistical noise on estimated OCC_{SRTM} was not remarkably smaller than in the SUVR methods, and became larger as the scan length became less (Fig. 7). Therefore, longer scan length is required compared with the SUVR methods.

In conclusion, the simplified method was applied to the measurement of the binding potential of DAT in a human study with ^{18}F-FE-PE2I. As well as SRTM, BP_{ND} estimated from SUVR of the target and reference regions using frames of late times provided stable estimates and showed good correlation with those by the conventional two-tissue compartment model, although they were greatly overestimated. In the estimation of transporter occupancy, SRTM with 90-min data is superior to the SUVR method, because it showed good linearity, less effect of cerebral blood flow, and higher reliability in the scan with small BP_{ND} after drug treatment. However, the SUVR method using late time frames also has the potential to provide transporter occupancy with a short scan length.

Acknowledgments We thank the staff of the clinical research support section, the clinical neuroimaging team, and the radiopharmaceutical production team at the molecular imaging center, National Institute of Radiological Sciences for their assistance in conducting the PET studies.

Compliance with ethical standards

Conflict of interest The authors declare that they have no conflict of interest.

References

1. Rinne JO, Ruottinen H, Bergman J, Haaparanta M, Sonninen P, Solin O. Usefulness of a dopamine transporter PET ligand [^{18}F]β-CFT in assessing disability in Parkinson's disease. J Neurol Neurosurg Psychiatry. 1999;67(6):737–41.
2. Ginovart N, Lundin A, Farde L, Halldin C, Bäckman L, Swahn CG, et al. PET study of the pre- and post-synaptic dopaminergic markers for the neurodegenerative process in Huntington's disease. Brain. 1997;120(3):503–14.
3. Jucaite A, Fernell E, Halldin C, Forssberg H, Farde L. Reduced midbrain dopamine transporter binding in male adolescents with attention-deficit/hyperactivity disorder: association between striatal dopamine markers and motor hyperactivity. Biol Psychiatry. 2005;57(3):229–38.
4. Arakawa R, Ichimiya T, Ito H, Takano A, Okumura M, Takahashi H, et al. Increase in thalamic binding of [11C]PE2I in patients with schizophrenia: a positron emission tomography study of dopamine transporter. J Psychiatr Res. 2009;43(15):1219–23.
5. Halldin C, Erixon-Lindroth N, Pauli S, Chou YH, Okubo Y, Karlsson P, et al. [^{11}C]PE2I: a highly selective radioligand for PET examination of the dopamine transporter in monkey and human brain. Eur J Nucl Med Mol Imaging. 2003;30(9):1220–30.
6. Varrone A, Steiger C, Schou M, Takano A, Finnema SJ, Guilloteau D, et al. In vitro autoradiography and in vivo evaluation in cynomolgus monkey of [^{18}F]FE-PE2I, a new dopamine transporter PET radioligand. Synapse. 2009;63(10):871–80.
7. Jucaite A, Odano I, Olsson H, Pauli S, Halldin C, Farde L. Quantitative analyses of regional [^{11}C]PE2I binding to the dopamine transporter in the human brain: a PET study. Eur J Nucl Med Mol Imaging. 2006;33(6):657–68.
8. Hirvonen J, Johansson J, Teräs M, Oikonen V, Lumme V, Virsu P, et al. Measurement of striatal and extrastriatal dopamine transporter binding with high-resolution PET and [^{11}C]PE2I: quantitative modeling and test-retest reproducibility. J Cereb Blood Flow Metab. 2008;28(5):1059–69.
9. DeLorenzo C. Kumar JSD., Zanderigo F, Mann JJ, Parsey RV. Modeling considerations for in vivo quantification of the dopamine transporter using [^{11}C]PE2I and positron emission tomography. J Cereb Blood Flow Metab. 2009;29(7):1332–45.
10. Seki C, Ito H, Ichimiya T, Arakawa R, Ikoma Y, Shidahara M, et al. Quantitative analysis of dopamine transporters in human brain using [^{11}C]PE2I and positron emission tomography: evaluation of reference tissue models. Ann Nucl Med. 2010;24(4):249–60.
11. Shetty HU, Zoghbi SS, Liow JS, Ichise M, Hong J, Musachio JL, et al. Identification and regional distribution in rat brain of radiometabolites of the dopamine transporter PET radioligand [^{11}C]PE2I. Eur J Nucl Med Mol Imaging. 2007;34(5):667–78.
12. Varrone A, Tóth M, Steiger C, Takano A, Guilloteau D, Ichise M, et al. Kinetic analysis and quantification of the dopamine transporter in the nonhuman primate brain with ^{11}C-PE2I and ^{18}F-FE-PE2I. J Nucl Med. 2011;52(1):132–9.
13. Sasaki T, Ito H, Kimura Y, Arakawa R, Takano H, Seki C, et al. Quantification of dopamine transporter in human brain using PET with ^{18}F-FE-PE2I. J Nucl Med. 2012;53(7):1065–73.
14. Ito H, Hietala J, Blomqvist G, Halldin C, Farde L. Comparison of the transient equilibrium and continuous infusion method for quantitative PET analysis of [^{11}C]raclopride binding. J Cereb Blood Flow Metab. 1998;18(9):941–50.
15. Lammertsma AA, Hume SP. Simplified reference tissue model for PET receptor studies. NeuroImage. 1996;4(3 Pt 1):153–8.
16. Farde L, Wiesel FA, Halldin C, Sedvall G. Central D_2-dopamine receptor occupancy in schizophrenic patients treated with antipsychotic drugs. Arch Gen Psychiatry. 1988;45(1):71–6.
17. Logan J, Fowler JS, Volkow ND, Ding YS, Wang GJ, Alexoff DL. A strategy for removing the bias in the graphical analysis method. J Cereb Blood Flow Metab. 2001;21(3):307–20.
18. Schou M, Steiger C, Varrone A, Guilloteau D, Halldin C. Synthesis, radiolabeling and preliminary in vivo evaluation of [^{18}F]FE-PE2I, a new probe for the dopamine transporter. Bioorg Med Chem Lett. 2009;19(16):4843–5.
19. Nordstrom AL, Farde L, Wiesel FA, Forslund K, Pauli S, Halldin C, et al. Central D2-dopamine receptor occupancy in relation to antipsychotic drug effects: a double-blind PET study of schizophrenic patients. Bioi Psychiatry. 1993;33(4):227–35.
20. Nyberg S, Farde L, Eriksson L, Halldin C, Eriksson B. 5-HT_2 and D_2 dopamine receptor occupancy in the living human brain: a PET study with risperidone. Psychopharmacology. 1993;110(3):265–72.
21. Nakashima Y, Farde L. Comparison of currently applied methods for PET quantification of specific [^{11}C]raclopride binding. J Cereb Blood Flow Metab. 1995;15:S643.
22. Brooks DJ, Ibanez V, Sawle GV, Playford ED, Quinn N, Mathias CJ, et al. Striatal D_2 receptor status in patients with Parkinson's disease, striatonigral degeneration, and progressive supranuclear

palsy, measured with ^{11}C-raclopride and positron emission tomography. Ann Neurol. 1992;31(2):184–92.
23. Rinne JO, Laihinen A, Rinne UK, Nagren K, Bergman J, Ruotsalainen U. PET study on striatal dopamine D_2 receptor changes during the progression of early Parkinson's disease. Mov Disord. 1993;8(2):134–8.
24. Volkow ND, Fowler JS, Wang GJ, Dewey SL, Schlyer D, MacGregor R, et al. Reproducibility of repeated measures of carbon-11-raclopride binding in the human brain. J Nucl Med. 1993;34(4):609–13.
25. Lammertsma AA, Bench CJ, Hume SP, Osman S, Gunn K, Brooks DJ, et al. Comparison of methods for analysis of clinical [^{11}C]raclopride studies. J Cereb Blood Flow Metab. 1996;16(1):42–52.
26. Farde L, Eriksson L, Blomquist G, Halldin C. Kinetic analysis of central [^{11}C]raclopride binding to D_2-dopamine receptors studied by PET–a comparison to the equilibrium analysis. J Cereb Blood Flow Metab. 1989;9(5):696–708.